



# Exosomes derived from M2-type microglia ameliorate oxygen-glucose deprivation/reoxygenation-induced HT22 cell injury by regulating miR-124-3p/NCOA4-mediated ferroptosis

Ke Xie <sup>a,1</sup>, Yun Mo <sup>b,1</sup>, Erli Yue <sup>a</sup>, Nan Shi <sup>a</sup>, Kangyong Liu <sup>a,\*</sup>

<sup>a</sup> Department of Neurology, Shanghai University of Medicine & Health Sciences Affiliated Zhoupu Hospital, No. 1500 Zhouyuan Road, Pudong New District, Shanghai, 201318, China

<sup>b</sup> Department of Neurology, Guizhou Medical University, China

## ARTICLE INFO

### Keywords:

M2 microglia-derived exosome  
OGD/R  
HT22 cells  
miR-124-3p

## ABSTRACT

**Background:** Although it has been reported that miRNA carried by M2 microglial exosomes protects neurons from ischemia–reperfusion brain injury, the mechanism of action remains poorly understood. This study aimed to explore the miRNA signaling pathway by which M2-type microglia-derived exosomes (M2-exosomes) ameliorate oxygen–glucose deprivation/reoxygenation (OGD/R)-induced cytotoxicity in HT22 cells.

**Methods:** BV2 microglia were induced by M2 polarization. Then, M2-exosomes were identified via transmission electron microscopy and special biomarker detection and co-cultured with HT22 cells. Cell proliferation was evaluated using the Cell Counting Kit-8 (CCK-8) assay. Intracellular concentrations of reactive oxygen species (ROS), Fe<sup>2+</sup>, glutathione (GSH), and malondialdehyde (MDA) were determined using dichlorofluorescein fluorescence and biochemical determination. miR-124-3p levels were determined using qRT-PCR, and protein expressions were examined via western blotting.

**Results:** OGD/R suppressed the proliferation and induced the accumulation of Fe<sup>2+</sup>, ROS, and MDA and reduction of GSH in mouse HT22 cells, suggesting ferroptosis of HT22 cells. OGD/R-induced changes in the above mentioned indexes was ameliorated by M2-exosomes but restored by the exosome inhibitor GW4869. M2-exosomes with (mimic-exo) or without miR-124-3p (inhibitor-exo) promoted and suppressed proliferation and ferroptosis-associated indexes of HT22 cells, respectively. Moreover, mimic-exo and inhibitor-exo inhibited and enhanced NCOA4 expression in HT22 cells, respectively. NCOA4 overexpression reversed the protective effects of miR-124-3p mimic-exo in OGD/R-conditioned cells. NCOA4 was targeted and regulated by miR-124-3p.

**Conclusions:** M2-exosome protects HT22 cells against OGD/R-induced ferroptosis injury by transferring miR-124-3p and NCOA4 into HT22 cells, with the latter being a target gene for miR-124-3p.

\* Corresponding author.

E-mail address: [lkylky136@163.com](mailto:lkylky136@163.com) (K. Liu).

<sup>1</sup> the author contributes equally to this work.

<https://doi.org/10.1016/j.heliyon.2023.e17592>

Received 14 January 2023; Received in revised form 19 June 2023; Accepted 21 June 2023

Available online 28 June 2023

2405-8440/© 2023 Published by Elsevier Ltd.

This is an open access article under the CC BY-NC-ND license

(<http://creativecommons.org/licenses/by-nc-nd/4.0/>).

## 1. Introduction

Ischemic stroke inevitably leads to physiological brain cell dysfunction and subsequent cell death. Although intravascular intervention can be performed to remove the thrombus and restore the blood flow, this procedure induces neuronal ischemia–reperfusion (I/R) injury. The most striking pathological feature of I/R injury is the excessive intracellular aggregation of reactive oxygen species (ROS) due to oxygen introduction after restoring the blood flow [1]. ROS-mediated lipid peroxidation, inflammatory response, and other series of events can lead to tight junction interruption and BBB disruption, which are the key pathological mechanisms of I/R injury [1,2]. Previous studies have demonstrated that oxidative stress causes neuronal apoptosis and necrosis in animal models of I/R and in vitro cell experiments [3–5]. Notably, recent studies have suggested that another mode of regulated non-apoptotic cell death, namely ferroptosis, also promotes I/R-induced neuronal loss [6,7]. Ferroptosis is a non-apoptotic, peroxide-driven modulated mode of cell death that depends on plentiful and easily obtained intracellular ROS and iron. The existence of this form of cell death had remained unknown until its recent discovery using pharmacological methods [8]. However, the mechanisms by which I/R regulates neuronal ferroptosis remain obscure.

Microglia are macrophages in the brain that function as a critical regulator of brain cell death and damage repair caused by brain injury through indirect secretion of nutritional factors or direct cell–cell communication and are the first line of defense against I/R injury [9]. Continuous ischemia and hypoxia induce microglia activation and recruitment toward the damaged area to remove debris and initiate the repair process [10]. Microglia are highly plastic cells that obtain specific phenotypes and features by reacting to specific stimuli. Microglia possess functional plasticity and dual phenotypes, namely proinflammatory M1 and anti-inflammatory M2 phenotypes [11]. M2 microglia is thought to be beneficial as they secrete anti-inflammatory mediators or chemokines to inhibit excessive inflammatory responses and promote the damaged neuron repair [9]. Inducing M2 microglia to secrete exosomes in vitro can improve ischemic brain injury [12]. Exosomes can be characterized as extracellular vesicles that transport microRNA (miRNA) to recipient cells [13]. Previous evidence suggests that the miRNA carried by M2 microglial exosomes protects neurons from ischemic and I/R brain injury [12]. However, the underlying mechanism is poorly understood.

MiRNA, a type of non-coding RNA molecule with approximately 20 nucleotides, mediates various cellular physiological events, such as proliferation and differentiation of cells and regulation of activation/inactivation of innate immune cells [14]. MiRNAs are usually encapsulated and transported by exosomes to impact the physiological process of recipient cells [13]. MiRNA-124 is a brain-specific miRNA expressed in microglia [15]. MiR-124 participates in the pathological progress of ischemic brain injury and protects neurons [16,17]. Moreover, miR-124 inhibits I/R injury and regulates ROS production in a rat model of I/R [18]. Increasing miR-124 levels can reverse oxygen-glucose deprivation/reoxygenation (OGD/R)-induced cell injury [19]. Recent studies have reported that miR-124 expression is significantly upregulated in the microglia of traumatic brains and exosomes of M2 microglia exposed to I/R [20,21]. In addition, M2 microglia-derived exosomes have been reported to possess neuroprotective effects against ischemic stroke, suggesting their potential as a therapeutic target for treating ischemic stroke [22]. However, the effects of M2 microglial exosomes containing miR-124 on ferroptosis in I/R-induced neuron injury as well as the underlying mechanisms remain unknown.

Bioinformatics analysis in the early stage have revealed that miR-124 can bind to a considerable number of mRNAs, including nuclear receptor coactivator 4 (NCOA4), a cargo receptor for ferritinophagy. NCOA4 has been reported to be closely related to lipid peroxidation, ferritinophagy, and ferroptosis by regulating the amount of bioavailable intracellular labile iron pools [23,24]. In addition, NCOA4 knockdown has been reported to markedly ameliorate ferritinophagy caused by I/R injury and inhibit ferroptosis [25]. However, the regulatory effects of miR-124 on NCOA4 have not been reported in ischemic stroke and other diseases. In the present study, we co-cultured M2 microglial exosomes and a HT22 cell model of OGD/R injury to elucidate the effects of M2 microglia exosomes on ferroptosis in OGD/R-induced HT22 cell injury and explore the mechanisms by which M2-exosomes containing miR-124-3p/NCOA4 relieve OGD/R-induced injury in HT22 cells.

## 2. Materials and methods

### 2.1. Cell culture and conditional treatment

HT22 (a mouse hippocampal neuronal cell line) and BV2 (a mouse microglial cell line) cells were used in this study. These cells were provided by the cell bank of Shanghai Biology Institute (Shanghai, China). DMEM (Trueline, Kaukauna, WI, USA) was used as the cell culture medium and mixed with 10% fetal bovine serum, 1% penicillin/streptomycin, and 2 mM L-glutamine (Solarbio, Beijing, China). The cells were cultured in a 5% CO<sub>2</sub> atmosphere at 37 °C. *In vitro* cerebral I/R was simulated through OGD/R treatment with 4 h of OGD conditional culture in a hypoxia chamber followed by 24 h of reperfusion culture in a normoxic incubator. To induce M2-type microglial differentiation, BV2 cells were cultured in a medium containing recombinant protein IL-4 (Re-IL-4) and identified via flow cytometry by detecting positive biomarkers (ARG and CD206).

### 2.2. Cell co-culture

HT22 cells and M2-type microglial cells were co-cultured in a Transwell permeable supports (Corning, Tewksbury, MA). M2-type microglial cells were seeded in the top chamber, whereas HT22 cells were seeded in the lower chamber. These two cell types were separated by a 0.4 μm porous membrane. Approximately 8 h before the start of co-culture, GW4869 (10 μM, Sigma, CA, USA) dissolved in DMSO was added into the top chamber to reduce exosomes release from M2-type microglial cells.

### 2.3. Exosome isolation

M2 microglial exosomes were acquired from approximately  $3.2 \times 10^7$  cells using an ExoQuick exosome precipitation solution (System Bioscience, USA) according to the manufacturer's instructions. In brief, M2 microglial cells were cultured for 24–48 h in  $\alpha$ -MEM with exosome depletion. Thereafter, the medium was collected and centrifugated at  $70,000 \times g$  overnight. The supernatant was then collected and further centrifuged for 1 h at  $70,000 \times g$ . After washing with phosphate-buffered saline (PBS), the exosome-containing pellet was centrifuged at  $70,000 \times g$  for 1 h and resuspended in 200  $\mu$ L of PBS. The prepared exosomes were stored at  $-80^\circ\text{C}$ . Exosomes were verified using specific protein markers, CD63 and TSG101, via western blotting with their antibodies (ab134045 and ab125011; Abcam, UK) and morphological examination using transmission electron microscopy (TEM).

### 2.4. Exosome uptake assay

This experiment sought to determine whether HT22 cells uptake M2 microglial exosomes. Exosomes were stained with PKH67 (Sigma, USA) according to the procedures described in a previous study [26] and then diluted in PBS with 0.5 mL of Diluent C. The labeled exosomes were subjected to 1 h of centrifugation at  $100,000 \times g$ . The exosome pellet was collected and resuspended in PBS. For the uptake experiment, labeled exosomes were added to the medium of HT22 cells. After 12, 24, or 48 h of co-culture, HT22 cell staining was performed using DAPI (Sigma, USA) and observed under a confocal microscope.

### 2.5. Evaluation of HT22 cell proliferation using CCK-8 assay

To determine cell proliferation, a CCK-8 assay was performed using the Cell Counting Kit-8 (CCK-8) (Signalway Antibody, USA). After different conditional treatments, HT22 cells were added into the CCK-8 solution (1:10) and incubated for 1 h. The optical densities of each cell sample were detected at a wavelength of 450 nm on a microplate reader (Pulangxin, Beijing, China). Each experiment was conducted in triplicate. Three cell tests were performed for each treatment.

### 2.6. qRT-PCR

The total RNA samples used for qRT-PCR were obtained from lysates of differently treated cells using TRIzol Reagent (Invitrogen, USA). The first step involved the reverse transcription of RNA using a cDNA synthesis kit (Invitrogen, USA). In the second step, the cDNA product obtained as a result of the reverse transcription was subjected to a real-time PCR procedure. The process steps were as follows: 10 min at  $95^\circ\text{C}$  followed by 40 cycles at  $95^\circ\text{C}$  for 15 s and  $45^\circ\text{C}$  for 45 s at  $60^\circ\text{C}$ . The relative expressions of each gene were calculated using the  $2^{-\Delta\Delta\text{Ct}}$  method and normalized to U6 (for microRNA) or  $\beta$ -actin (for mRNA). The following primers were used: ARG, F: 5'-GGTGGGTGGTCTGGTATC-3', R: 5'-CATTGCCATCCTATCCTG-3'; CD206, F: 5'-CTGCTTCTGGCTTTTATCTC-3', R: 5'-ATGGCACTTA-GAGCGTCC-3'; mmu-miR-124-3p, F: 5'-GCGTAAGGCACGCGGTG-3', R: 5'-AGTGCAGGGTCCGAGGTATT-3'; NCOA4, F: 5'-AAAT-CAGTGTCCGTCCCC-3', R: 5'-CAGATTTAGGTTCCATAGGC-3'; GAPDH, F: 5'-GTGTTTCTCTCGTCCCGTAG-3', R: 5'-TTAGTGG-GTCTCGTCC-3'; and U6, F: 5'-CTCGCTTCGGCAGCAC-3', R: 5'-AACGCTTCACGAATTTGCGT-3'. Data were expressed as the average of three replicates.

### 2.7. Western blotting

The total protein samples used for western blotting were obtained from lysates of differently treated cells using RIPA lysis buffer (Thermo Fisher Scientific, USA) and quantified using a Pierce™ BCA Protein Assay Kit (Thermo Fisher Scientific, USA). Equal amounts (25  $\mu$ g) of protein samples were loaded onto a 10% acrylamide gel for SDS-PAGE according to molecular weight. Proteins from the gel were transferred to a nitrocellulose membrane (Millipore, USA) through electrophoresis. The membrane was blocked for 1 h with 5% nonfat dry milk. Overnight incubation with specific antibodies (NCOA4, bs-19051R, Bioss, USA; GAPDH, #5174, CST; TSG101, Ab125011, Abcam, UK; CD63, Ab59479, Abcam, UK) at  $4^\circ\text{C}$  and 1 h incubation with a secondary antibody (Beyotime, China) at  $37^\circ\text{C}$  were performed in the same order. The blot on the membrane was visualized using a chemiluminescence system (Tanon, China). GAPDH expression level was used as the control.

### 2.8. Biochemical determination and intracellular ROS measurement in HT22 cells

Intracellular concentrations of  $\text{Fe}^{2+}$ , GSH, and MDA were determined using iron assay kit (ab83366, Abcam), GSH kit (A006-2, Nanjing Jiancheng bioengineering Institute, China), and MDA kit (A003-1, Nanjing Jiancheng bioengineering Institute, China), respectively, according to the manufacturer's instructions.

Intracellular ROS was detected according to a method described in a previous study [27]. After 24 h of culture, cells were immersed in PBS containing 20  $\mu$ M 2',7'-dichlorodihydrofluorescein diacetate and kept for 20 min at  $37^\circ\text{C}$ . Subsequently, the cells were treated with OGD/R or OGD/R in combination with M2 microglial exosomes and then incubated with 200  $\mu$ M of  $\text{H}_2\text{O}_2$  in PBS. After treatment, the cells were collected for determination of intracellular ROS concentration using an inverted fluorescence microscope. Three fields of each photomicrograph were preserved. The amount of intracellular ROS was evaluated based on fluorescence intensity on Image-Pro Plus 6.0 (Media Cybernetics, USA).

## 2.9. NCOA4 overexpression in HT22 cells

A lentiviral vector (pLVX-puro) recombined with the full-length human NCOA4 gene coding region (CDS) sequence was used for NCOA4 overexpression (oeNCOA4), and the mock vector was used as the negative control (oeNC). oeNCOA4 or oeNC was transduced into the cells using Lipofectamine™ 2000 Transfection Reagent (Thermo Fisher Scientific, USA) according to the manufacturer's instructions. After 48 h of transfection, the cells were harvested for further analysis.

## 2.10. Dual luciferase reporter gene analysis

Binding site prediction for miR-124-3p and NCOA4 was conducted using the TargetScan and Starbase databases. Based on the predicted binding site, wild and mutant sequences were synthesized and cloned into luciferase reporter vectors (pGL3-Basic). Those luciferase reporter vectors together with miR-124-3p inhibitor or mimics were transfected into HT22 cells. The cells were cultured for another 48 h and harvested for luciferase activity analysis using the dual luciferase reporter gene test kit (Yuanpinghao Biotechnology Co, China).

## 2.11. Statistical analysis

Data were presented as mean  $\pm$  standard deviation (SD) for at least three samples. All data analyses were conducted using GraphPad Prism software (La Jolla, USA; Version 7.0). Comparison among three or more groups was performed using one-way analysis of variance. Significant differences between two groups were determined using *t*-test. *P* value of  $<0.05$  was considered statistically significant.

## 3. Results

### 3.1. OGD/R suppressed the proliferation and promoted the accumulation of ROS and Fe<sup>2+</sup> in mouse HT22 cells

After 24 and 48 h of OGD/R treatment, HT22 cell proliferation was significantly suppressed (Fig. 1A). Ferroptosis is a ROS-dependent cell death mode associated with two biochemical features, namely iron accumulation and lipid peroxidation. Our results showed that HT22 cells treated with OGD/R for 48 h had increased concentrations of ROS (Fig. 1B) and Fe<sup>2+</sup> (Fig. 1C). GSH, a member of the antioxidant system, was downregulated (Fig. 1D). MDA, a product of lipid peroxidation, was significantly upregulated (Fig. 1E).

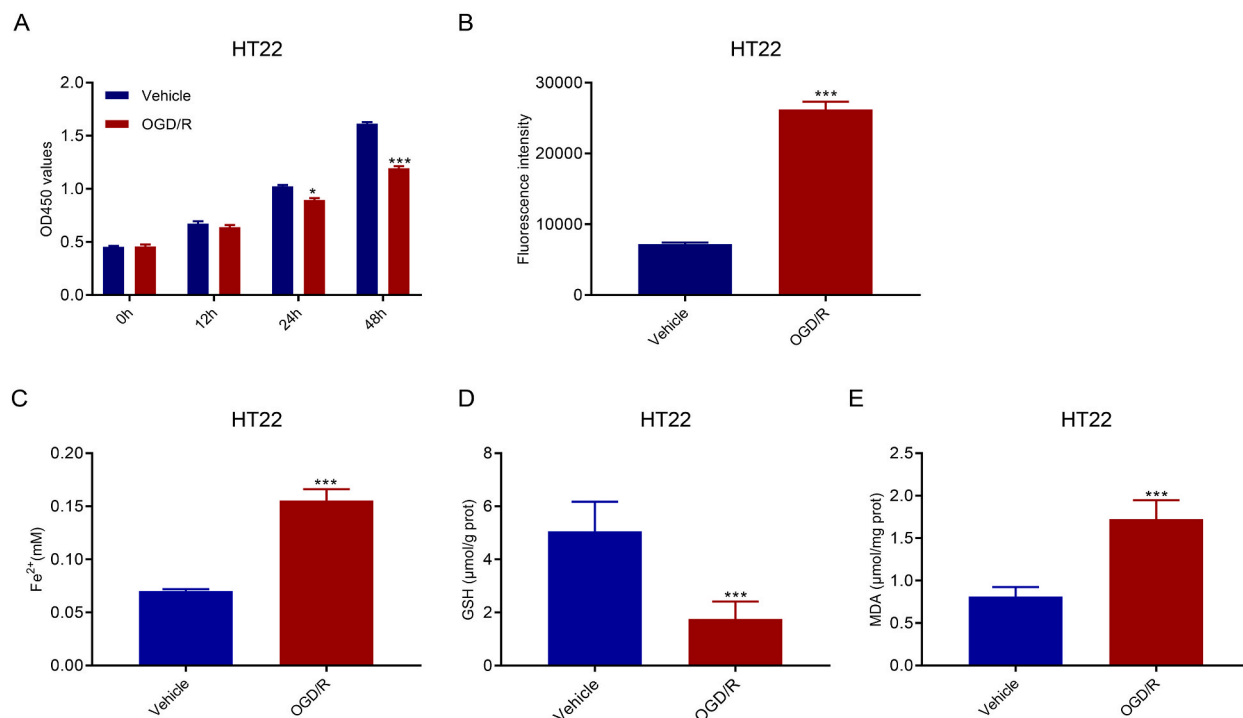


**Fig. 1.** OGD/R suppressed proliferation and promoted ROS accumulation in HT22 cells. A. CCK-8 assay demonstrated the suppressed proliferation of HT22 cells after OGD/R treatment. B–E. In such OGD/R-conditioned HT22 cells, ROS accumulation increased (B), Fe<sup>2+</sup> concentrations increased (C), GSH concentrations decreased (D), and MDA concentrations increased (E). \**p* < 0.05, \*\*\**p* < 0.001 vs. vehicle.

Overall, these findings suggest that OGD/R treatment causes ferroptosis of HT22 cells.

### 3.2. M2-type microglia-derived exosomes ameliorated OGD/R-induced injury in mouse HT22 cells

HT22 cells and M2-type microglial cells were co-cultured in a Transwell system to explore the effects of M2-type microglia-derived exosomes on OGD/R-induced cytotoxicity in HT22 cells. Fig. 2A shows that compared with OGD/R alone, co-culturing for 48 h promoted greater cell proliferation; however, this increase was reduced by the exosome inhibitor GW4869. After 48 h of culturing, cells were harvested to determine the concentrations of ROS and  $\text{Fe}^{2+}$ . As shown in Fig. 2B, M2-type microglial cells co-culturing promoted significantly lower ROS levels compared with OGD/R alone in HT22 cells; however, this decrease was reversed by the exosome inhibitor GW4869. Similarly, the increased intracellular  $\text{Fe}^{2+}$  levels induced by M2-type microglial cell co-culturing was reversed by the exosome inhibitor GW4869 (Fig. 2C). The reduced GSH levels and increased MDA levels induced by M2-type microglial cells co-culturing were also reversed by the exosome inhibitor GW4869 (Fig. 2D and E). These data indicate that M2-type microglia-derived exosomes play a protective role against OGD/R-induced cytotoxicity in HT22 cells.

### 3.3. M2-exosomes contributed to the recovery of OGD/R-induced mouse HT22 cell injury by delivering miR-124-3p

To explore the potential downstream pathway of miR-124-3p by which M2-exosomes alleviated OGD/R-induced HT22 cell injury, M2-exosomes with miR-124-3p overexpression (mimic-exo) or miR-124-3p silencing (inhibitor-exo) were isolated from M2-type microglia transduced with miR-124-3p mimics or miR-124-3p inhibitor. Mimic-exo or inhibitor-exo and OGD/R were then co-cultured with HT22 cells. After co-culturing for 24 and 48 h, miR-124-3p inhibitor-exo promoted a markedly lower cell proliferation than the control. Moreover, after 48 h of co-culturing, miR-124-3p mimic-exo promoted greater cell proliferation than OGD/R (Fig. 3A). Subsequent analysis of ferroptosis-related biochemical features showed that ROS and  $\text{Fe}^{2+}$  aggregation was suppressed by mimic-exo co-culturing but was facilitated by inhibitor-exo co-culturing (Fig. 3B and C); GSH level was increased by mimic-exo co-culturing but decreased by inhibitor-exo co-culturing (Fig. 3D); and MDA level was decreased by mimic-exo co-culturing but increased by inhibitor-exo co-culturing (Fig. 3E). Furthermore, qRT-PCR and western blotting revealed that NCOA4 mRNA and protein expression in HT22 cells were inhibited by mimic-exo co-culturing and enhanced by inhibitor-exo co-culturing (Fig. 3F and G).

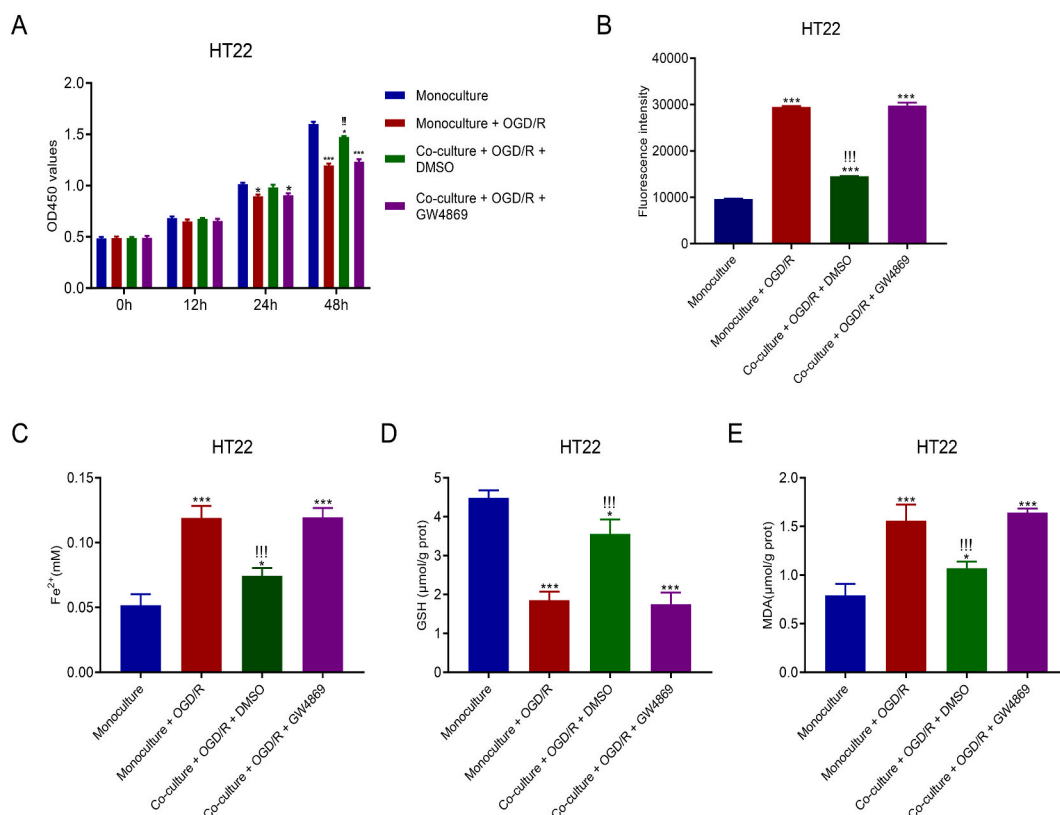


**Fig. 2.** M2-type microglial cell co-culturing ameliorated ferroptosis in HT22 cells injured by OGD/R. A. OGD/R-stimulated HT22 cells showed increased proliferation after co-culturing with M2-type microglial cells. B–E. In co-cultured HT22 cells, ROS accumulation was suppressed (B),  $\text{Fe}^{2+}$  concentrations were reduced (C), GSH concentrations were increased (D), and MDA levels were decreased (E). \* $p < 0.05$ , \*\*\* $p < 0.001$  vs. monoculture, !!! $p < 0.001$  vs. monoculture + OGD/R.

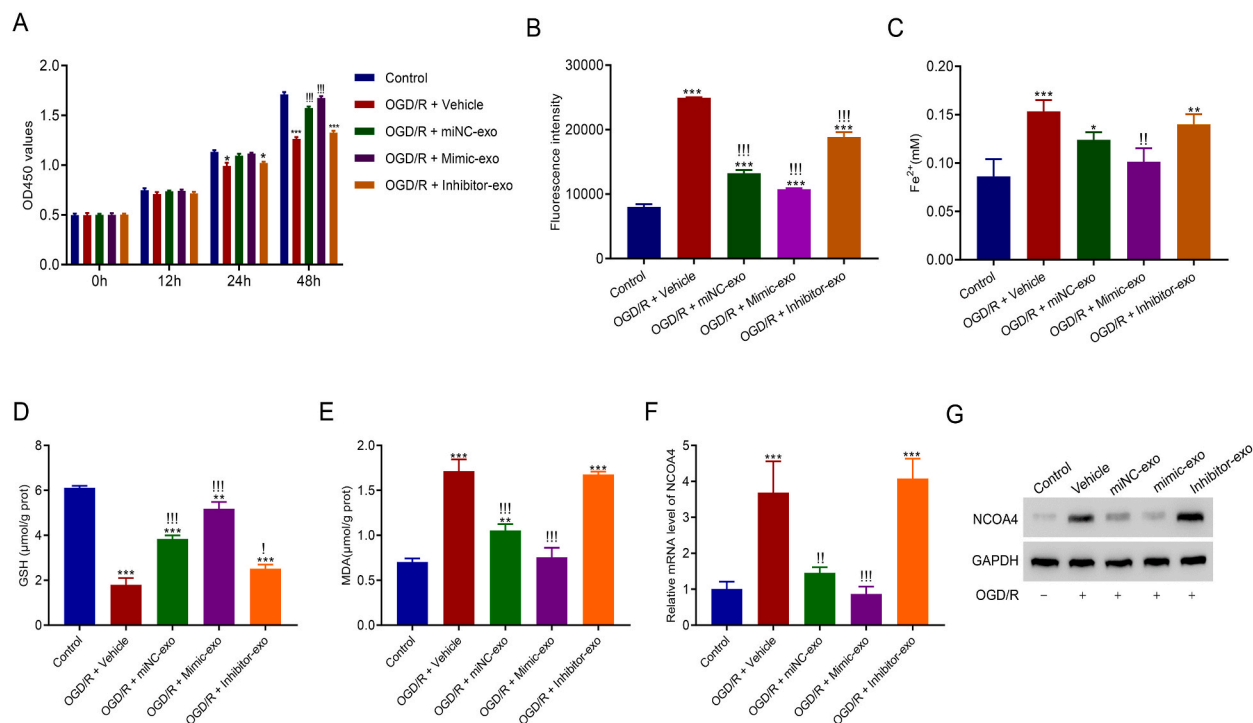


**Fig. 3.** M2-exosomes contributed to the recovery of OGD/R-induced injury in HT22 by delivering miR-124-3p. A. Co-culture of miR-124-3p mimic-exo promoted OGD/R cell proliferation. B. ROS accumulation was decreased in OGD/R-conditioned HT22 cells after co-culturing with miR-124-3p mimic-exo. C. Fe<sup>2+</sup> concentration in OGD/R-induced HT22 cells was downregulated after co-culturing with mimic-exo. D. Mimic-exo upregulated GSH levels in OGD/R-conditioned cells. E. MDA levels in OGD/R-conditioned cells were downregulated in OGD/R-induced HT22 cells after co-culturing with miR-124-3p mimic mimic-exo. F and G. NCOA4 expressed low levels of mRNA and protein after OGD/R-conditioned cells were treated with mimic-exo. Please see Supplemental files to find uncropped pictures. \*p < 0.05, \*\*p < 0.01, \*\*\*p < 0.001 vs. control; !p < 0.05, !!p < 0.01, !!!p < 0.001 vs. vehicle.

### 3.4. NCOA4 overexpression suppressed mimic-exo function in OGD/R-conditioned cells

To examine the participation of NCOA4 in the protective role of miR-124-3p-overexpressed exosomes in OGD/R-conditioned cells, NCOA4 was overexpressed in HT22 cells by overexpression vector transfection (oeNCOA) (Fig. 4A and B). NCOA4 overexpression reduced cell proliferation and significantly suppressed pro-proliferative function of M2-exosomes in OGD/R-conditioned cells after 24 and 48 h of co-culturing (Fig. 4C). After 48 h of co-culturing, ferroptosis-related biochemical features of HT22 cells were analyzed. Fig. 4D and E shows that NCOA4 overexpression increased ROS and Fe<sup>2+</sup> levels and reversed the inhibitory effects of M2-exosomes on ROS and Fe<sup>2+</sup> production in OGD/R cells. Furthermore, M2-exosomes suppressed NCOA4 expression in OGD/R-conditioned cells (Fig. 4F).

### 3.5. MiR-124-3p decreased NCOA4 expression by binding to its 3'UTR

To explore the regulatory role of miR-124-3p in NCOA4 expression, miR-124-3p was silenced or overexpressed in HT22 cells transduced by an inhibitor or mimic. Notably, miR-124-3p silencing increased NCOA4 mRNA and protein expressions, whereas miR-124-3p overexpression decreased these expressions (Fig. 5A and B), suggesting the repressive impact of miR-124-3p on NCOA4 expression. Bioinformatics prediction suggested that miR-124-3p had binding sites on the NCOA4 3'-UTR. To determine whether miR-124-3p targets NCOA4, luciferase report plasmids containing wild NCOA4 3'-UTR or mutant NCOA4 3'-UTR were constructed (Fig. 5C). These luciferase report plasmids together with miR-124-3p inhibitor or mimic were used to transduce HT22 cells. Luciferase activity analysis showed that miR-124-3p overexpression decreased, but miR-124-3p silencing increased, the luciferase activity of cells with wild NCOA4 3'-UTR transfection, whereas miR-124-3p did not affect the luciferase activity of cells with mutant NCOA4 3'-UTR transfection. These results indicate that miR-124-3p targets and controls NCOA4 expression (Fig. 5D).

M2-type microglia were preliminarily identified by the surface antigen CD206 using CD206 anti-body. Figure S1A shows the IHC images of microglia stained with CD206. Furthermore, the IHC images of HT22 cells with NCOA4 staining before/after OGD/R treatment, and with/without exosome incubation are shown in Figure S1B.

M2-type microglia were observed after BV2 cells were stimulated by Re-IL-4. Figure S2A shows that the M2-type microglia-specific biomarkers ARG and CD26 were upregulated in Re-IL-4-induced cells. Figure S2B and Figure S2C show that after Re-IL-4 induction,

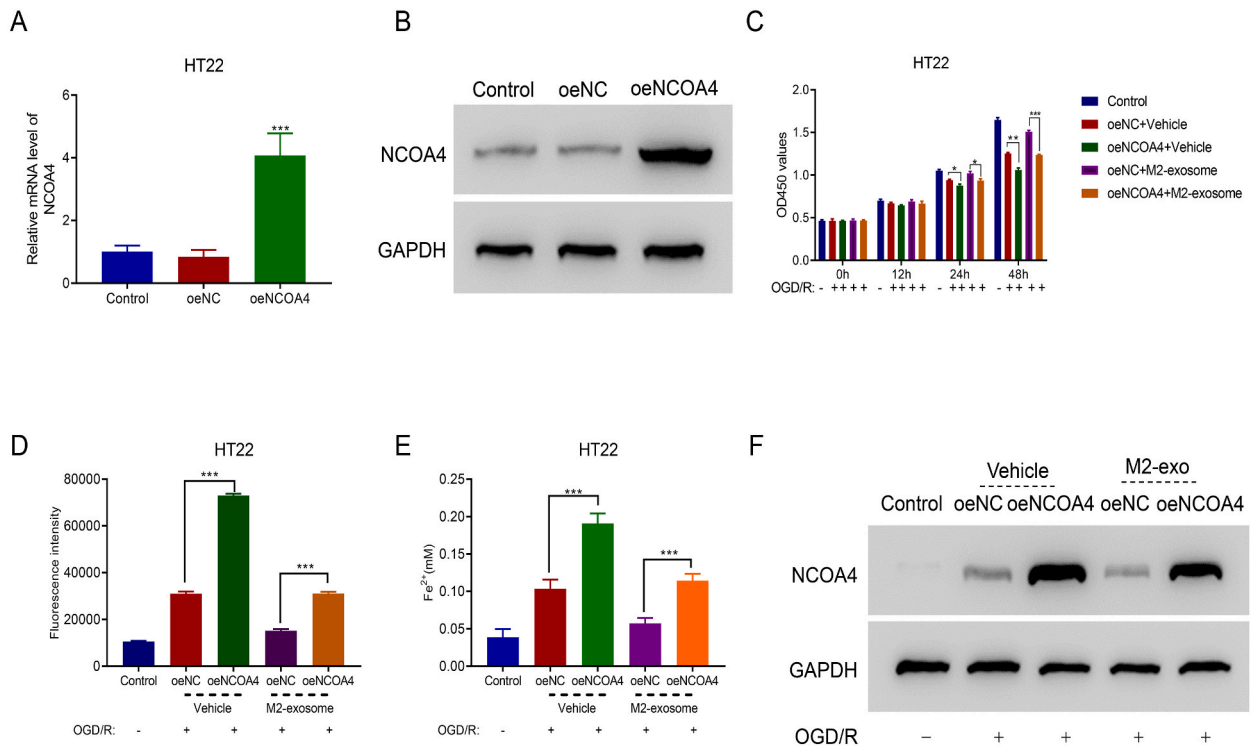


**Fig. 4.** NCOA4 overexpression suppressed mimic-exo function in OGD/R-conditioned HT22 cells. A and B. NCOA4 expression at the mRNA and protein levels was upregulated by NCOA4 overexpression vector (oeNCOA4) transduction. \*\*\* $p < 0.001$  vs. oeNC. Please see Supplemental files to find uncropped pictures. C. NCOA4 overexpression suppressed the proliferation of M2-exo-treated OGD/R cells. \* $p < 0.05$ , \*\* $p < 0.001$ , \*\*\* $p < 0.001$ . D and E. ROS and  $Fe^{2+}$  accumulation in M2-exo-cultured OGD/R-conditioned cells was upregulated after transfecting with oeNCOA4. \*\*\* $p < 0.001$ . F. oeNCOA4 overexpression elevated NCOA4 protein expression. Please see Supplemental files to find uncropped pictures.

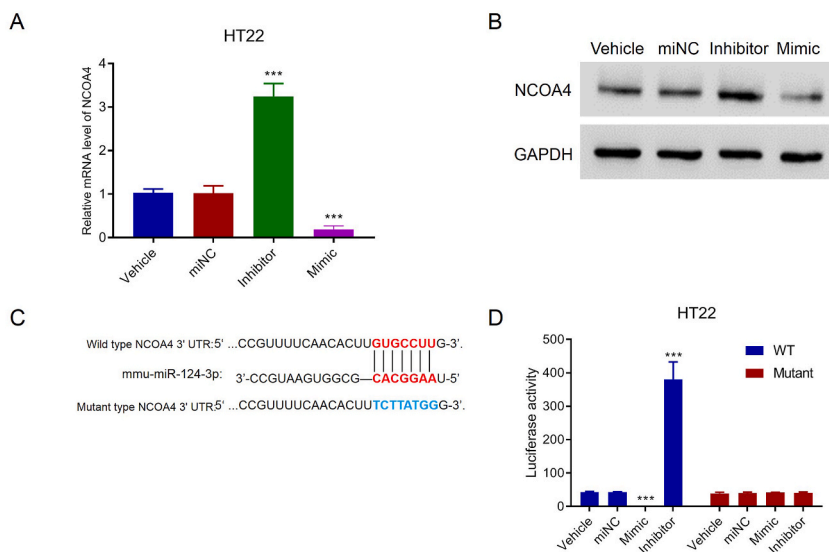


**Fig. 5.** miR-124-3p suppressed NCOA4 expression by binding to the 3'UTR in HT22 cells. A and B. NCOA4 expression increased and decreased the levels of mRNA and protein in HT22 cells transduced by miR-124-3p inhibitor and mimic, respectively. Please see Supplemental files to find uncropped pictures. C. Wild-type and mutant binding sites between has-miR-124-3p and NCOA4 3'UTR. D. The mutant binding site strongly suppressed the binding between miR-124-3p and NCOA4 in HT22 cells. \*\*\* $p < 0.001$  vs. miNC.

ARG-positive cells accounted for 87.8% of the total number of cells. M2-type microglia-derived exosomes were isolated to determine miR-124-3p expression level. Figure S2D shows that miR-124-3p expression was upregulated in M2 microglial exosomes. Furthermore, miR-124-3p was overexpressed and silenced in M2 microglial cells transfected with the corresponding mimic and inhibitor (Figure S2E). To verify the M2 microglial exosome, TEM was used to observe the morphology of the exosome (Figure S2F), which showed the increased expression levels of the specific biomarkers TSG101 and CD63 (Figure S2G). Consistent with M2-BV2 cells transfected with a mimic and inhibitor, the obtained M2-exosomes contained increased and decreased levels of miR-124-3p (Figure S2H). The PKH-67 staining assay indicated that M2-exosomes were absorbed by HT22 cells through endocytosis (Figure S2I).

#### 4. Discussion

Severe cell injury and death are pathological indicators of cerebral I/R; therefore, regulating the modulated mode of cell death can prevent or reverse I/R injury. The present study verified that M2 microglia-derived exosomes deliver miR-124-3p to HT22 neuronal cells and protect cells injured by OGD/R from ferroptosis, indicating their potential as a therapeutic target for I/R-induced neuron injury.

A sudden reduction in available oxygen and nutrients is a key factor for cellular damage in ischemic or hypoxic tissues. At this point, a cascade reaction of stress and death occurs in cells, and disorder of the endogenous mechanisms responsible for ROS clearance promote the accumulation of ROS [28]. ROS accumulation, a common phenomenon associated with cell I/R damage, has been observed in OGD/R culture of multiple types of cells in vitro, including neuronal cells and microglia [29]. The present study also supports this phenomenon as ROS levels sharply increased in OGD/R conditional HT22 cells. ROS accumulation is closely associated with controlled cell death [30]. With the current understanding of ferroptosis, which can be described as a mechanism of regulated cell death controlled by ROS and iron accumulation, some studies have observed ferroptosis in neurons injured by OGD/R [31,32]. In our results, ROS and  $\text{Fe}^{2+}$  levels and lipid peroxidation products were significantly increased in HT22 cells after 48 h of OGD/R treatment. Therefore, consistent with other studies showing that OGD/R caused neuronal ferroptosis [31,33], our study revealed that OGD/R caused ferroptosis in the hippocampal neuronal cell line HT22.

Long before the concept of ferroptosis had been proposed, several studies found abnormalities in iron accumulation and iron metabolism in ischemic regions of the brain [34,35]. Iron deposition is positively correlated with the poor prognosis of ischemic stroke [36]. In 2012, Dixon et al. proposed the concept of “ferroptosis” [8]; since then, some studies have gradually revealed that the form of ferroptosis characterized by excessive intracellular accumulation of labile iron is an important factor for cerebral I/R injury [37,38]. Our results potentially support the role of ferroptosis, an iron-dependent modulated form of cell death, in the pathologic progression of cerebral I/R injury. The relationship between ferroptosis and cerebral I/R injury remains to be explored given that the exact mechanism of iron death is yet to be elucidated.

MiR-124, a miRNA molecule with high M2 microglia content, plays a protective role against ischemia-related neuronal injury through exosomes as a communication medium between cells [39,40]. For instance, brain extracts from traumatic brain injury increase the level of miR-124 in BV2 exosomes, and such miR-124 enriched BV2 exosomes promote neuronal cell survival [41]. M2 microglial exosomes carrying miR-124 were intravenously injected to reduce infarct size and promote neuronal survival in mouse models of ischemic brain injury [9]. MiR-124-3p delivered via microglia exosomes protects neuronal cells by influencing modulated cell survival, such as autophagy [41]. Our results demonstrate for the first time that ferroptosis of HT22 cells induced by OGD/R was abrogated by miR-124-3p overexpressed M2 microglial exosomes.

As a regulatory ncRNA, miRNA post-transcriptionally regulates gene expression by obstructing messenger RNA (mRNA) translation or facilitating mRNA degradation [42]. Our data prove that miR-124-3p targets NCOA4 mRNA and regulates NCOA4 expression. NCOA4, a selective cargo receptor, functions conservatively across cell types, thereby contributing to the balance in intracellular iron levels by regulating the autophagic degradation of ferritin. Given the central role of NCOA4 in regulating intracellular iron levels, recent studies have shown that ferroptosis sensitivity is modulated by NCOA4 [23,24]. Ferroptosis can be suppressed when NCOA4 deletion induces the blockage of ferritinophagy and ferritin degradation; in contrast, ferroptosis is easily induced when NCOA4 is overexpressed [24]. NCOA4 is involved in various ferroptosis-related pathologic conditions, including neurodegenerative diseases, I/R injury, and cancer [23]. In the present study, NCOA4 overexpression abrogated the protective effects of miR-124-3p against ferroptosis in OGD/R-conditioned HT22 cells, suggesting that miR-124-3p might target NCOA4 to protect the cell from ferroptosis in OGD/R conditional HT22 cells. This has been proven by luciferase reporter assays and functional experiments wherein miR-124-3p targeted and suppressed NCOA4 expression.

Exosomes contain parts of identical components with the parent cells, and could serve as ideal cell-free therapy. The present study revealed that M2 microglial exosomes could ameliorate neuron ferroptosis in HT22 cells exposed to OGD/R, suggesting a simple and economical method to treatment I/R injury-based cerebrovascular disease. Moreover, abnormal miR-124-3p/NCOA4 expression might indicate the degree of cerebrovascular disorder; however, further clinical and experimental studies are needed to confirm this finding.

#### 5. Conclusions

The present study showed the protective function of M2 microglial exosomes against neuron ferroptosis in a HT22 cell model of OGD/R-induced injury. The underlying mechanism for this was the ability of M2 microglial exosomes to deliver miR-124-3p to HT22 cells, thereby suppressing the expression of NCOA4 in HT22 cells and consequently eliminating intracellular  $\text{Fe}^{2+}$  and ROS accumulation. The protective effects of M2 microglia might have been caused by the synergistic effects of multiple components in the exosomes; more in vitro and in vivo studies are needed to prove this. Nonetheless, miR-124-3p/NCOA4 could be an effective

therapeutic target for preventing and reversing I/R-induced neuron loss. Our findings provided new insights into the pathogenesis of I/R injury-based cerebrovascular disorders and propose a potential therapeutic strategy.

### Ethics approval and consent to participate

All experimental protocols were approved by Shanghai University of Medicine & Health Sciences Affiliated Zhoupu Hospital. There were no any animal experiments or human samples in this study.

### Consent for publication

All the authors are consent for publication this paper.

### Author contribution statement

Ke Xie: Performed the experiments; Contributed reagents, materials, analysis tools or data; Wrote the paper. Yun Mo: Performed the experiments; Analyzed and interpreted the data. Erli Yue, Nan Shi: Performed the experiments. Kangyong Liu: Conception and design; Contributed reagents, materials, analysis tools or data; Analyzed and interpreted the data; Wrote the paper.

### Funding statement

Ke Xie was supported by the Key Disciplines Construction Foundation of Health Commission of Pudong New District of China {PWZxk2017-25}, the Natural Science Foundation of Shanghai {17ZR1425800}.

### Data availability statement

Data will be made available on request.

### Declaration of competing interest

The authors declare the following financial interests/personal relationships which may be considered as potential competing interests: Ke Xie reports financial support was provided by Key Disciplines Construction Foundation of Health Commission of Pudong New District of China (No. PWZxk2017-25). Ke Xie reports financial support was provided by Natural Science Foundation of Shanghai (No.17ZR1425800). Kangyong Liu reports financial support was provided by Scientific Research Project of Shanghai Municipal Health Commission (202150015).

### Appendix A. Supplementary data

Supplementary data to this article can be found online at <https://doi.org/10.1016/j.heliyon.2023.e17592>.

### References

- [1] K. Mandalanieni, A. Rayi, D.V. Jillella, in: *StatPearls, Stroke Reperfusion Injury*, Treasure Island (FL), 2022.
- [2] D.N. Granger, P.R. Kvietys, Reperfusion injury and reactive oxygen species: the evolution of a concept, *Redox Biol.* 6 (2015) 524–551.
- [3] J. Wang, et al., Nox2 and Nox4 participate in ROS-induced neuronal apoptosis and brain injury during ischemia-reperfusion in rats, *Acta Neurochir. Suppl.* 127 (2020) 47–54.
- [4] R. He, et al., Curcumin-laden exosomes target ischemic brain tissue and alleviate cerebral ischemia-reperfusion injury by inhibiting ROS-mediated mitochondrial apoptosis, *Mater Sci Eng C Mater Biol Appl* 117 (2020), 111314.
- [5] Y. Dai, et al., Isoquercetin attenuates oxidative stress and neuronal apoptosis after ischemia/reperfusion injury via Nrf2-mediated inhibition of the NOX4/ROS/NF- $\kappa$ B pathway, *Chem. Biol. Interact.* 284 (2018) 32–40.
- [6] X. Guan, et al., Galangin attenuated cerebral ischemia-reperfusion injury by inhibition of ferroptosis through activating the SLC7A11/GPX4 axis in gerbils, *Life Sci.* 264 (2021), 118660.
- [7] X. Guan, et al., The neuroprotective effects of carvacrol on ischemia/reperfusion-induced hippocampal neuronal impairment by ferroptosis mitigation, *Life Sci.* 235 (2019), 116795.
- [8] S.J. Dixon, et al., Ferroptosis: an iron-dependent form of nonapoptotic cell death, *Cell* 149 (5) (2012) 1060–1072.
- [9] Y. Song, et al., M2 microglia-derived exosomes protect the mouse brain from ischemia-reperfusion injury via exosomal miR-124, *Theranostics* 9 (10) (2019) 2910–2923.
- [10] P. Surinkaew, et al., Role of microglia under cardiac and cerebral ischemia/reperfusion (I/R) injury, *Metab. Brain Dis.* 33 (4) (2018) 1019–1030.
- [11] A.A. Atta, et al., Microglia polarization in nociceptive pain: mechanisms and perspectives, *Inflammopharmacology* 31 (3) (2023) 1053–1067.
- [12] D. Zhang, et al., Microglia exosomal miRNA-137 attenuates ischemic brain injury through targeting Notch1, *Aging (Albany NY)* 13 (3) (2021) 4079–4095.
- [13] M. Groot, H. Lee, Sorting mechanisms for MicroRNAs into extracellular vesicles and their associated diseases, *Cells* 9 (4) (2020) 1044.
- [14] Y. Bronevetsky, K.M. Ansel, Regulation of miRNA biogenesis and turnover in the immune system, *Immunol. Rev.* 253 (1) (2013) 304–316.
- [15] A.J. Svahn, et al., miR-124 Contributes to the functional maturity of microglia, *Dev Neurobiol* 76 (5) (2016) 507–518.
- [16] S. Hamzei Taj, et al., MiRNA-124 induces neuroprotection and functional improvement after focal cerebral ischemia, *Biomaterials* 91 (2016) 151–165.
- [17] Y. Sun, et al., MicroRNA-124 protects neurons against apoptosis in cerebral ischemic stroke, *CNS Neurosci. Ther.* 19 (10) (2013) 813–819.

- [18] Y. Wu, J. Yao, K. Feng, miR-124-5p/NOX2 Axis modulates the ROS production and the inflammatory microenvironment to protect against the cerebral I/R injury, *Neurochem. Res.* 45 (2) (2020) 404–417.
- [19] K. Shu, Y. Zhang, Protodioscin protects PC12 cells against oxygen and glucose deprivation-induced injury through miR-124/AKT/Nrf2 pathway, *Cell Stress Chaperones* 24 (6) (2019) 1091–1099.
- [20] X. Ge, et al., Increased microglial exosomal miR-124-3p alleviates neurodegeneration and improves cognitive outcome after rmTBI, *Mol. Ther.* 28 (2) (2020) 503–522.
- [21] S. Huang, et al., Increased miR-124-3p in microglial exosomes following traumatic brain injury inhibits neuronal inflammation and contributes to neurite outgrowth via their transfer into neurons, *FASEB J* 32 (1) (2018) 512–528.
- [22] J. Zang, et al., Inhibition of PDE1-B by vinpocetine regulates microglial exosomes and polarization through enhancing autophagic flux for neuroprotection against ischemic stroke, *Front. Cell Dev. Biol.* 8 (2020), 616590.
- [23] N. Santana-Codina, J.D. Mancias, The role of NCOA4-mediated ferritinophagy in Health and disease, *Pharmaceuticals* 11 (4) (2018) 114.
- [24] W. Hou, et al., Autophagy promotes ferroptosis by degradation of ferritin, *Autophagy* 12 (8) (2016) 1425–1428.
- [25] C. Li, et al., Nuclear receptor coactivator 4-mediated ferritinophagy contributes to cerebral ischemia-induced ferroptosis in ischemic stroke, *Pharmacol. Res.* 174 (2021), 105933.
- [26] G. Wei, et al., Dendritic cells derived exosomes migration to spleen and induction of inflammation are regulated by CCR7, *Sci. Rep.* 7 (2017), 42996.
- [27] X. Wankun, et al., Protective effect of paeoniflorin against oxidative stress in human retinal pigment epithelium in vitro, *Mol. Vis.* 17 (2011) 3512–3522.
- [28] L. Minutoli, et al., ROS-mediated NLRP3 inflammasome activation in brain, heart, kidney, and testis ischemia/reperfusion injury, *Oxid. Med. Cell. Longev.* 2016 (2016), 2183026.
- [29] L. Li, et al., Ferroptosis is associated with oxygen-glucose deprivation/reoxygenation-induced Sertoli cell death, *Int. J. Mol. Med.* 41 (5) (2018) 3051–3062.
- [30] L.J. Su, et al., Reactive oxygen species-induced lipid peroxidation in apoptosis, autophagy, and ferroptosis, *Oxid. Med. Cell. Longev.* 2019 (2019), 5080843.
- [31] Y. Yuan, et al., Kaempferol ameliorates oxygen-glucose deprivation/reoxygenation-induced neuronal ferroptosis by activating nrf2/SLC7A11/GPX4 Axis, *Biomolecules* 11 (7) (2021) 923.
- [32] G. Chen, et al., Hydroxysafflor yellow A and anhydrosafflor yellow B alleviate ferroptosis and parthanatos in PC12 cells injured by OGD/R, *Free Radic. Biol. Med.* 179 (2021) 1–10.
- [33] Z. Hui, et al., Compound Tongluo Decoction inhibits endoplasmic reticulum stress-induced ferroptosis and promoted angiogenesis by activating the Sonic Hedgehog pathway in cerebral infarction, *J. Ethnopharmacol.* 283 (2022), 114634.
- [34] Y. Kondo, et al., Regional differences in late-onset iron deposition, ferritin, transferrin, astrocyte proliferation, and microglial activation after transient forebrain ischemia in rat brain, *J. Cerebr. Blood Flow Metabol.* 15 (2) (1995) 216–226.
- [35] U.J. Park, et al., Blood-derived iron mediates free radical production and neuronal death in the hippocampal CA1 area following transient forebrain ischemia in rat, *Acta Neuropathol.* 121 (4) (2011) 459–473.
- [36] M.D.C. Valdes Hernandez, et al., Association between striatal brain iron deposition, microbleeds and cognition 1 Year after a minor ischaemic stroke, *Int. J. Mol. Sci.* 20 (6) (2019) 1293.
- [37] Z.Q. Bu, et al., Emerging role of ferroptosis in the pathogenesis of ischemic stroke: a new therapeutic target? *ASN Neuro* 13 (2021), 17590914211037505.
- [38] P. Wang, et al., Mitochondrial ferritin attenuates cerebral ischaemia/reperfusion injury by inhibiting ferroptosis, *Cell Death Dis.* 12 (5) (2021) 447.
- [39] Z. Li, et al., M2 microglial small extracellular vesicles reduce glial scar formation via the miR-124/STAT3 pathway after ischemic stroke in mice, *Theranostics* 11 (3) (2021) 1232–1248.
- [40] Y. Yang, et al., MiR-124 enriched exosomes promoted the M2 polarization of microglia and enhanced Hippocampus neurogenesis after traumatic brain injury by inhibiting TLR4 pathway, *Neurochem. Res.* 44 (4) (2019) 811–828.
- [41] D. Li, et al., Increases in miR-124-3p in microglial exosomes confer neuroprotective effects by targeting FIP200-mediated neuronal autophagy following traumatic brain injury, *Neurochem. Res.* 44 (8) (2019) 1903–1923.
- [42] M. Correia de Sousa, et al., Deciphering miRNAs' action through miRNA editing, *Int. J. Mol. Sci.* 20 (24) (2019) 6249.